GEOPHYSICAL RESEARCH LETTERS, VOL. 23, NO. 19, PAGES 2621-2624, SEPTEMBER 15, 1996

Evidence of secular changes in rainfall data from the tropical western and central Pacific over a 20-year period

Jose A. Maliekal and Thomas J. Petroski

Department of the Earth Sciences, SUNY College at Brockport

Abstract. Rainfall data from the tropical western and central Pacific over the period from 1971 to 1990 show both decadal and interannual variability. A statistically significant secular trend may be used to model the overall rainfall variability. However, locally weighted regression analysis reveals that this increasing trend stalls in the early 1980's, and reverses its course by the year 1990. Decomposition of individual rainfall time series into low frequency, seasonal, and irregular components facilitates the isolation of the time varying annual cycle and the elucidation of the interannual signal. Strong or prolonged warm El Niño-Southern Oscillation events dominate the interannual variability during the study period. The decadal scale variation in the annual cycle is so systematic, in fact, there is approximately a 20% reduction in its amplitude between 1971 and 1982. In addition, the long-term change in the seasonal component appears to modulate the much shorter-term interannual signal.

Introduction

Several recent studies have reported enhancements of the moisture content in the lower troposphere [*Hense et al., 1988; Gaffen et al., 1991; Gutzler, 1992*], and the hydrological cycle in the tropics over the warmest oceans *[Flohn and Kapala, 1989]*. Regional and worldwide variations in the sea surface temperature, including a recent warming trend in the tropics, have also been observed [*Folland et al., 1984; Nitta and Yamada, 1989; Flohn and Kapala, 1989*]. Apparently, the moistening of the lower troposphere has its "roots" in the surface temperature of the warmest oceans *[Graham 1995]*. The underlying hypothesis postulates that the observed rising trend in the tropospheric moisture and temperature [*Hansen and Lebedeff, 1988; Angell, 1990; Jones, 1994*], especially the sharp rises since the mid-1970's, is due to the contemporaneous enhancement of the tropical hydrological cycle forced by the increase in the sea surface temperature [*Flohn and Kapala, 1989; Graham, 1995*]. Supporting evidence, though indirect, comes from the outgoing longwave radiation (OLR) data, which suggest an enhancement of the convective activity in the equatorial Pacific Ocean near the dateline region [*Nitta and Yamada, 1989; Graham, 1995*]. Rainfall data alone can provide direct support.

We have used monthly rainfall data *[Morrissey et al., 1995]* from the tropical western and central Pacific islands and atolls (Table I), over the period from 1971 to 1990, to examine the nature of the regional hydrological cycle. The Pacific "warm pool", where the water temperature is in excess of 27.5° C, encircles vast majority of these atolls and islands [*Sadler et al., 1987*]. Accordingly, convection in this region is likely to produce high, cold cloud tops [*Flohn and Kapala, 1989*]. Monsoonal westerlies (on the equatorward side of the monsoon trough), the Inter-tropical Convergence Zone (ITCZ), and the South Pacific Convergence Zone (SPCZ), help establish cumulus convection in this region (Fig. 1).

Paper number 96GL02387
0094-8534/96/96GL-02387$05.00

Exploratory Analysis

Principal component analysis (PCA) is often employed to separate "signals" in a data set from "noise". In the context of the present study, the goal of PCA is to summarize the space/time variations in the rainfall data set in terms of a few linear combinations of the individual rainfall time series. The resulting principal components are similar to weighted averages, and describe temporal variations. Weights are the elements of the eigenvectors of the covariance matrix of rainfall time series. Because of the scaling convention, it is the squares of the weights that sum to unity. Consequently, the signs of the individual elements of eigenvectors (or the signs of the weights) are not unique. Therefore, each principal component can illustrate the presence of a secular trend, but it cannot stipulate the direction of that trend. Nevertheless, the sign and magnitude of the weights contain information about the contribution of the observations from a particular location to the corresponding principal component.

We applied PCA to rainfall time series, $X(t)$, and rainfall anomaly time series $X_A(t)$. The first principal components explain 28% and 22% of the variances, respectively. Taken individually, other principal components account for much less variability, and as such, we focus only on the first principal component.

In the first principal component of the rainfall series (Fig. 2a), the El Niño-Southern Oscillation (ENSO) signal is mixed with the annual cycle. Sea surface temperature data from the tropical Pacific also show similar behavior [*Wang, 1993*]. The corresponding eigenvector pattern (Table I) is closely related to the timing of the peak in the rainy season. The eight westernmost stations within the Mariana and Micronesian islands, where the rainfall maxima occur in the boreal summer, have the same sign. All other stations have their rainfall maxima in the austral spring or summer; they have the opposite sign. The statistically significant (at the 95% confidence) linear trend fitted to this principal component, with a slope of 0.83 mm month^{-1}, seems to indicate an overall increase in the regional rainfall.

By comparison, the four major warm ENSO events (1972-73, 1976-77, 1982-83, and 1986-87) can easily be identified in the first principal component of the anomaly series (Fig. 2 b). The steeper slope (1.16 mm month^{-1}) of the statistically significant trend line of this principal component further highlights the overall increase in the rainfall. Several near-equatorial stations within the Kiribati and Tuvalu islands, where the ENSO related interannual variability is quite

Table I. List of stations, eigen vectors of rainfall [$X(t)$] and rainfall anomaly [$X_A(t)$] series, and slopes (mm month^{-1}) of regression lines.

No	Station	X(t)	X_A(t)	Slope
1	Palau	-0.15	-0.10	0.12
2	Yap	-0.17	-0.11	-0.14
3	Guam	-0.17	-0.07	-0.19
4	Guam, NAS	-0.17	-0.08	-0.14, #
5	Pohnpei	-0.18	-0.15	-0.16, #
6	Wake	-0.05	-0.01	-0.11, #
7	Kwajalein	-0.14	-0.04	-0.32, #
8	Banaba	0.21	0.28	0.11, #
9	Majuro	-0.13	-0.11	-0.40, #
10	Butaritari	0.13	0.18	0.18
11	Tarawa	0.19	0.28	0.11, #
12	Beru	0.14	0.24	0.01, #
13	Nanumea	0.30	0.35	0.25, #
14	Arorae	0.22	0.33	0.17, #
15	Nui	0.31	0.31	0.36, #
16	Niutao	0.31	0.37	0.42
17	Funafuti	0.21	0.17	0.51
18	Niulakita	0.16	0.04	0.05, #
19	Ha'apai	0.03	-0.08	-0.43, #
20	Vavau	0.09	-0.09	-0.38
21	Keppel	0.12	-0.04	-0.40, #
22	Apia	0.22	-0.02	-0.40
23	A. Samoa	0.15	0.02	0.05
24	Pukapuka	0.19	0.12	0.46
25	Niuafa'au	0.13	-0.01	-0.30, #
26	Rakahanga	0.20	0.17	0.42
27	Fanning	0.11	0.21	0.04, #
28	Rarotonga	0.05	-0.05	-0.05
29	Aitutaki	0.08	-0.04	-0.30, #
30	Penrhyn	0.25	0.26	0.71
31	Takaroa	0.11	0.09	0.42, #
32	Hereheretue	0.07	0.06	0.56, #
33	Hao	0.10	0.04	0.21, #

# indicates the presence of an inflection point in the locallyweighted regression curve.

pronounced, have larger positive weights (Table I). Obviously, the trend seen in the principal component is most pronounced here. The easternmost stations near 20°S (Polynesian islands) also share this trait. Climatologically,

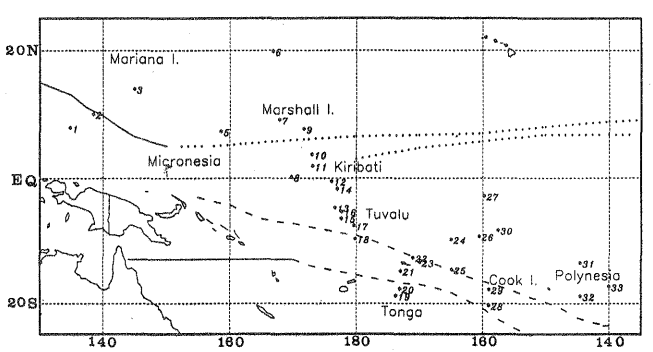

Figure 1. Station locations and January and July positions of the monsoon trough (full lines), SPCZ (dashed lines), and ITCZ (dotted lines) based on *Sadler et al. [1987]*. Stations are identified using serial numbers given in Table I. Poleward positions of the SPCZ and ITCZ represent summer conditions.

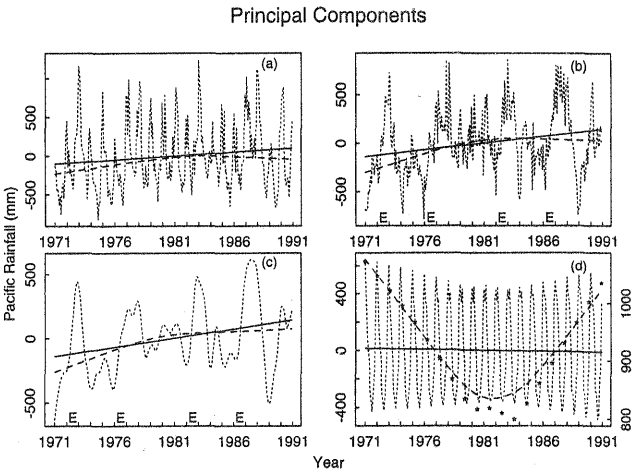

Figure 2. Principal Components of the (a) rainfall, (b) rainfall anomaly, (c) low frequency sub-series, and (d) seasonal sub-series. Full lines represent linear regression fit and dashed lines in (a), (b), and (c) represent weighted regression curves. In (d), * denotes the amplitude of the annual cycle, and the dashed line represents the weighted regression curve fitted to the amplitude. "E" represents the beginning of a warm ENSO event.

they are located to the east of the SPCZ. It is reasonable to conjuncture that the rainfall enhancement implied by the eigenvector pattern is due to an eastward shift in the position of the SPCZ, which is noted by *Morrissey and Graham [1996]* also. Stations within the Tongan islands and a few stations at the southern periphery of the Cook islands have negative weights like the westernmost stations in the Northern Hemisphere. The former group of islands is located in the vicinity of the SPCZ. An eastward displacement of the SPCZ may explain the decrease in rainfall suggested by the change in the sign of the weights. The Micronesian islands come under the influence of the northeast trades during the austral summer, and monsoon westerlies during the boreal summer. Interannual variations in the monsoon trough may explain the observed rainfall variability at this location.

In ordinary regression analysis, all points have equal weights, hence, "outliers" or "bad" values can seriously disturb the least squares fit [*Montgomery and Peck, 1982*]. A re-analysis of the above principal components using robust locally weighted regression [*Cleveland, 1979*] is performed to validate the linear trend. This procedure accommodates temporal changes represented by, $Y(t) = g(t)\ X(t) + \epsilon$, where $g(t)$ is an unknown smooth function. Results (Fig. 2a, b) reveal that the increasing trend is restricted to the first half of the study period, it halts in the early 1980's, and reverses direction by the year 1990.

For comparison, we also analyzed annual rainfall values from individual stations using ordinary regression and locally weighted regression. Slopes in Table I are computed after the unit normal scaling [*Montgomery and Peck, 1982*] of the regressor and response variables. About 60% of the stations have positive slopes, and 40% of the stations have the opposite conduct. Except for the four largest slopes, positive and negative slopes have comparable magnitudes. Therefore, the trends noticed in the principal components of the rainfall and rainfall anomaly series correspond to an overall increase in the rainfall of this region. Slopes of the regression lines and the weights of the first principal

component of the rainfall anomaly series have virtually identical signs. They also have similar magnitudes, except for the stations from the Tongan and Cook islands, where the negative slopes have larger magnitude than the negative weights. Although, both statistical techniques are capturing the same overall behavior, PCA underestimates the decreasing trend. Locally weighted regression curves of about 60% of the stations in both categories exhibit inflection points; they largely occur in the early 1980's. The flattening of the secular trend in the second half of the study period is just as pervasive as its increase in the first half.

It is clear that when a linear trend is used describe the variability of short rainfall time series, the ensuing characterization may paint a partial picture. *Cleveland et al. [1983]* describe an alternate methodology to study time series. It involves the decomposition of monthly time series into seasonal, trend or low frequency, and irregular components. They have used this technique to describe the variability of the atmospheric carbon dioxide.

Time Series Analysis

Each monthly rainfall time series, $X(t)$, is decomposed into three sub-series that vary differently through time, that is, $X(t) = T(t) + S(t) + I(t)$. The first of the component series, $T(t)$, describes the low frequency variability, which may include a trend or other modes of long-term change. The second component series, $S(t)$, consists of periodic or nearly periodic fluctuations related to the annual cycle. If the annual cycle is invariant with time, the seasonal component will contain exactly repeating oscillations. The last component series, $I(t)$, represents the leftover part after the determination of the low frequency and seasonal components.

Figure 3 shows an example of the three component series, the ENSO related variability is evident in the low frequency component (Fig.3b). Notice too the systematic variation in the annual cycle (Fig. 3c). Its amplitude decreases in the 1970's, reaches a minimum in the early 1980's, and increases thereafter. All 33 stations show systematic fluctuations, but the magnitudes involved are different. More than 80% of the stations record relative maxima in the early 1970's and late 1980's. At about 45% of the stations the minima occur in the early 1980's; it develops in the middle of the 1970's at 30% of the stations. A few stations have their minima in the middle part of the 1980's. A minimum is absent in fewer than 15% of the stations. The two stations with the largest slopes and the station with the smallest slope are among them. Besides this, the occurrence of the relative minimum in the seasonal sub-series bears no association with the direction of the secular trend discussed in the previous section.

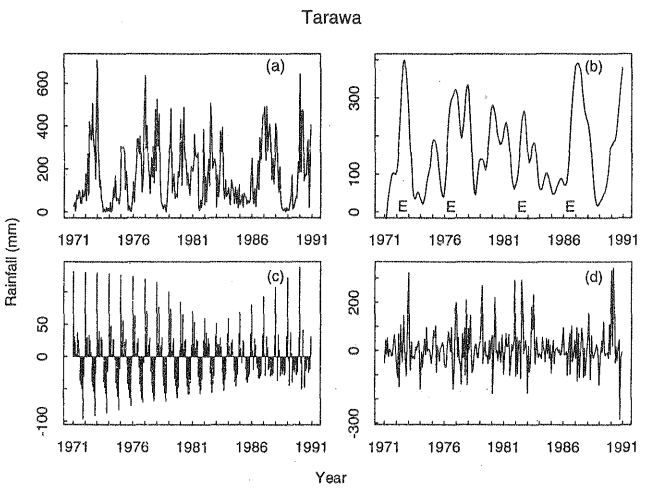

Figure 3. (a) Monthly time series of rainfall from Tarawa (1.21° N, 172.55° E) and its (b) low frequency, (c) seasonal, and (d) irregular sub-series. "E" represents the beginning of a warm ENSO event.

The first principal components of the low frequency and seasonal sub-series (Fig. 2c, d) respectively account for 47% and 60% of the variances. Since, the eigenvector of the seasonal (low frequency) sub-series is similar to that of the rainfall series (rainfall anomaly), their spatial patterns are similar. Hence, we have not included them in Table I, and the following discussion focuses only on the temporal structure. A statistically significant linear trend can be detected only in the principal component of the low frequency sub-series (Fig. 2c). Incidently, its slope (1.18 mm month^{-1}) is steeper than the slope of the rainfall anomaly series. The temporal pattern consists of four strong warm and one strong cold ENSO events. It is worth emphasizing that a smoother "rendition" of the first principal component of the anomaly series (Fig. 2b) would be indistinguishable from the temporal structure of the low-frequency sub-series (Fig. 2c).

The first principal component of the seasonal sub-series reveals slow and steady changes in the amplitude of the annual cycle. We highlight this by plotting the yearly range of the principal component (Fig. 2d). In the beginning, and at the end of the study period, the amplitude of the annual cycle is higher. Sandwiched between them is a distinct minimum, which according to the locally weighted regression takes place in the 1981-82 period. Between the maximum in the beginning and the above-mentioned minimum, the amplitude of the annual cycle changes by 20%. There is also asymmetry in the temporal structure. The seasonal maximum of the overall regional rainfall is in the austral summer. The decline in the amplitude of the annual cycle appears to be largely due to the reduction in the convective activity during this season.

Longer records, of course, are needed to specify the precise nature of the aforementioned variability. Based on the evidence presented here, it is clear that the underlying time scale is inter-decadal, which differ from the two to five-year recurrence interval of the ENSO phenomenon. The minimum in the amplitude of the first principal component of the seasonal sub-series (Fig. 2d) coincides with the flattening of the locally weighted regression curve fitted to the first principal components of the anomaly series (Fig. 2b), and low-frequency sub-series (Fig. 2c). It seems that, the inter-decadal changes in the amplitude of the seasonal variation of the hydrological cycle have a modulating influence on the interannual variability. When the amplitude of the annual cycle is on its declining mode, the low frequency variability is marked by the occurrence of strong warm ENSO events. Accordingly, rainfall activity in the western and central Pacific displays a rising trend.

Conclusions

The hydrological cycle in the tropical western and central Pacific exhibits interannual and decadal scale variability. On the whole, the strength of the hydrological cycle has increased since 1971. Both PCA and regression analysis suggest that the rising trend in rainfall is most pronounced in two zones: the

near-equatorial regions between 170°E and the dateline, and the South Pacific islands to the east of the climatological position of the SPCZ. Several northern hemispheric islands influenced by the monsoon westerlies, and southern hemispheric islands in the vicinity the SPCZ behave in the opposite manner. Locally weighted regression curves fitted to the principal components of monthly rainfall time series and rainfall anomaly series clarify that the aforementioned trends are restricted to the decade of the 1970's. This trend levels in the 1980's and reverses direction by 1990.

By and large, strong cold ENSO events are few in number between 1971 and 1988. In conjunction with warm ENSO events, equatorial convection and SPCZ are dislodged from their normal positions. As a result, the near-equatorial dateline region and the Polynesian islands experience increases in rainfall activity. Quite possibly, certain unique features, such as increased intensity, greater frequency, and extended longevity, of the warm ENSO events within the 1971 to 1988 period may explain the observed rainfall enhancement at these locations.

A systematic long-term variability exposed by the seasonal sub-series is by far the high point of our research. Between 1971 and 1981-82, the change in the amplitude of the annual cycle of the rainfall data is as much as 20%. This inter-decadal change appears to modulate the ENSO related interannual variability.

At this point of time, it is not prudent to speculate whether these secular changes are the result of feedback processes involving tropospheric carbon dioxide and water vapor, or part and parcel of the natural variability of the climate system. Analysis of longer time series and modeling studies are needed to tackle this issue. We would like to bring to the attention of those interested in climate change studies the inter-decadal change in the amplitude of the annual cycle and interannual variability exhibited by the hydrological cycle of the western and central Pacific.

Acknowledgments. This work is supported in part by NOAA grant NA46GP0219.

References

Angell, J. K., Variations in global tropospheric temperature after adjustment for the El Niño influence. *Geophys. Res. Lett., 17,* 1093-1096, 1990.

Cleveland, W. S., Robust locally weighted Regression and smoothing scatter plots, *J. Am. Stat. Assoc., 74,* 829-836, 1979.

Cleveland, W. S., A. E. Freeny, and T. E. Graedel, The seasonal component of atmospheric CO_2: Information from new approaches to the decomposition of seasonal time series, *J. Geophys. Res., 88,* 10,934-10,946, 1983.

Flohn, H., and A. Kapala, Changes in the tropical sea-air interaction processes over a 30-year period, *Nature, 338,* 244-246, 1989.

Folland, C. K., D. E. Parker, and F. E. Kates, Worldwide marine temperature fluctuations 1856-1981, *Nature, 310,* 670-673, 1984.

Gaffen, D. J., T. P. Barnett, and W. P. Elliott, Space and time scales of global tropospheric moisture, *J. Clim., 4,* 989-1008, 1991.

Graham, N. E., Simulation of recent global temperature trends, *Science, 267,* 666-671, 1995.

Gutzler, D. S., Climate variability of temperature and humidity over the tropical western pacific, *Geophys. Res. Lett., 19,* 1595-1598, 1992.

Hansen, J., and S. Lebedeff, Global surface temperatures: Update through 1987, *Geophys. Res. Lett., 15,* 323-326, 1988.

Hense, A. P., P. Krahe, and H. Flohn, Recent fluctuations of tropospheric temperature and water vapor content in the tropics, *Meteorol. Atmos. Phys., 38,* 215-227, 1988.

Jones, P. D., Recent warming in global temperature series, *Geophys. Res. Lett., 21,* 1149-1152, 1994.

Montgomery, D.C., and Peck, E.A., *Introduction to Linear Regression Analysis,* 504 pp., John Wiley & Sons, New York, 1982.

Morrissey, M. L, and N. E. Graham, 1996, Evidence of a recent decadal-scale climate shift in the tropical Pacific atmosphere-ocean system, *Bull. Amer. Met. Soc., 77,* 1207-1219, 1996.

Morrissey, M. L., M. A. Shafer, S. E. Postwako, and B. Gibson, The pacific rain gage rainfall database, *Water Resour. Res., 31,* 2111-2113, 1995.

Nitta, T., and S. Yamada, Recent warming of tropical sea surface temperature and its relationship to the northern hemisphere circulation, *J. Meteor. Soc. Japan, 67,* 375-383, 1989.

Sadler, J. C., M. A. Lander, A. M. Hori, and L. K. Oda, Tropical Marine Climatic Atlas, *Dep. of Meteorol.,* UHMET 87-02, 29 pp., University of Hawaii, Honolulu, Hawaii, 1987.

Wang, X. L., The coupling of the annual cycle and ENSO over the tropical Pacific, *J. Atmos. Sci., 58,* 1115-1136, 1993.

J. Maliekal and T. Petroski, Department of the Earth Sciences, SUNY College at Brockport, Brockport, NY 14420. (e-mail: jmalieka@weather.brockport.edu)

(Received April 26, 1996; revised July 10, 1996; accepted July 11, 1996)